Proceedings

Multi-dimensional measurements of the parton shower in p+p collisions at $\sqrt{s}$ = 200 GeV

Monika Robotkova [1,2,*] (for the STAR Collaboration)

[1] Nuclear Physics Institute of the CAS, Husinec - Rez, 130 Rez, 250 68, Czech Republic
[2] Czech Technical University in Prague, Faculty of Nuclear Sciences and Physical Engineering, Department of Physics Brehova 7, Praha, 115 19, Czech Republic
* Correspondence: ; robotkova@ujf.cas.cz

Abstract: Jets are collimated sprays of hadrons and can serve as an experimental tool for studying the dynamics of quarks and gluons. In particular, differential measurements of jet substructure observables enable a systematic exploration of the parton shower evolution. The SoftDrop grooming technique utilizes the angular ordered Cambridge/Aachen reclustering tree and provides a correspondence between the experimental observables, such as the shared momentum fraction (z_{g}), groomed jet radius or split opening angle (R_{g}), and the QCD splitting functions in vacuum. We present fully corrected correlations between z_{g} and R_{g} at the first split for jets of varying momenta and radii in p+p collisions at $\sqrt{s}$ = 200 GeV. To study the evolution along the jet shower, we also present the splitting observables at the first, second, and third splits along the jet shower for various jet and initiator prong momenta. As these novel measurements are presented in three dimensions, we outline the correction procedure so that its final version can be used as an inspiration for some of the future multi-differential measurements.

Keywords: jets, jet substructure, parton shower, SoftDrop, STAR

Citation: Robotkova, M. Multi-dimensional measurements of the parton shower in p+p collisions at $\sqrt{s}$ = 200 GeV. *Universe* **2024**, *1*, 0. https://doi.org/

Received:
Revised:
Accepted:
Published:

1. Introduction

In high-energy collisions, the evolution of hard scattered partons involves both parton showering and hadronization. Throughout this evolution, clusters of collimated hadrons emerge, referred to as jets, and their characteristics can be delineated through the application of jet clustering algorithms. In our analysis, we employ the anti-k_{T} [1] and Cambridge/Aachen (C/A) [2] algorithms. The exploration of jet substructure allows to study the inner dynamics of quarks and gluons within the jet. Investigating jet substructure enables a deeper comprehension of both perturbative processes (parton shower) and non-perturbative processes (hadronization), with grooming techniques like SoftDrop [3] providing valuable access to these phenomena.

The outcomes of the SoftDrop procedure yield two distinct observables known as the shared momentum fraction (z_{g}) and groomed radius (R_{g}). This technique is based on removing wide-angle radiation which does not pass the SoftDrop condition:

$$z_{\mathrm{g}} = \frac{\min(p_{\mathrm{T,1}}, p_{\mathrm{T,2}})}{p_{\mathrm{T,1}} + p_{\mathrm{T,2}}} > z_{\mathrm{cut}} \left(\frac{R_{\mathrm{g}}}{R}\right)^{\beta}, \quad (1)$$

where $p_{\mathrm{T,i}}$ denotes the transverse momentum of the associated subjet, while R represents the jet's resolution parameter, and R_{g} stands for the separation between the two subjets. Equation 1 involves two parameters, both set to specific values in our analysis: $\beta = 0$ and $z_{\mathrm{cut}} = 0.1$. The parameter z_{cut} functions as a momentum fraction cut, mitigating sensitivity to non-perturbative effects.

We introduce two approaches for investigating parton shower dynamics utilizing these observables: examining the correlation between z_g and R_g during the initial split, and tracking the evolution of substructure observables at the first, second, and third splits.

2. Correlation between z_g and R_g at the first split

Data used in this study were collected in p+p collisions at $\sqrt{s} = 200$ GeV by the STAR experiment [4] in 2012. A detailed description of the dataset and analysis cuts can be found in Ref. [5].

To obtain true particle-level distributions, we must correct the data for the detector inefficiency and the finite instrumental resolution. Our observables exist in a three-dimensional space ($p_{\mathrm{T,jet}}$, z_g, R_g), necessitating the application of multi-dimensional unfolding techniques[1]. We employ 2D Iterative Bayesian unfolding [6] to unfold the z_g vs. R_g and then we correct for the $p_{\mathrm{T,jet}}$ using projections and weights from $p_{\mathrm{T,jet}}$ response matrix. Additionally, corrections for trigger and jet finding efficiencies are incorporated into the analysis.

In Figure 1, the fully corrected z_g distributions are displayed for various corrected $p_{\mathrm{T,jet}}$ bins at $R = 0.4$. Each color corresponds to a distinct R_g bin, and the bands surrounding the data points indicate systematic uncertainties. Notably, we observe a strong dependence of z_g on R_g, while the influence of $p_{\mathrm{T,jet}}$ appears negligible. The z_g distributions exhibit an increasing steepness with larger R_g, suggesting an enhancement in softer wide-angle splitting.

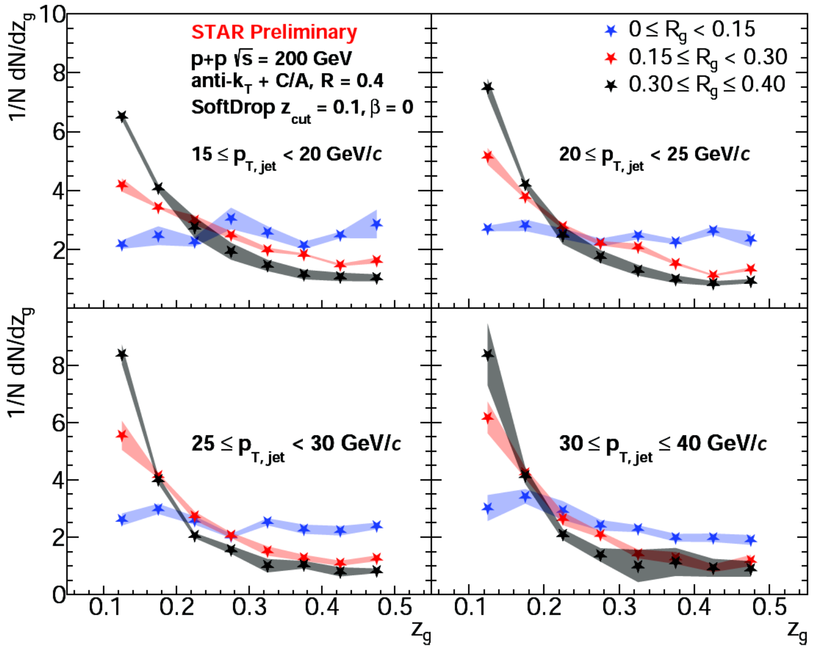

Figure 1. Fully corrected z_g distributions for three R_g bins for jets with $R = 0.4$ in p+p collisions at $\sqrt{s}$ = 200 GeV. Individual panels correspond to different $p_{\mathrm{T,jet}}$ intervals (see legend).

3. Evolution of the splitting kinematics along the jet shower

In the latter part of our investigation, we delve into the evolution of substructure observables at the first, second, and third splits. The dataset utilized remains consistent with the description in Section 2. To explore multiple splits beyond the first one, we employ a specialized variant of the SoftDrop technique known as iterative SoftDrop [7].

Similarly to the previous scenario, the data must be unfolded in a 3-dimensional space. In this context, the dimensions involve z_g vs. $p_{\mathrm{T,jet}}$ vs. split number, and R_g vs. $p_{\mathrm{T,jet}}$ vs.

[1] This technique will be amended in the final paper.

split number. Utilizing the 2D Iterative Bayesian unfolding technique, we unfold either z_g or R_g vs. $p_{T,jet}$, and subsequently construct a hierarchy matrix with particle-level splits on the x-axis and detector-level splits on the y-axis. The unfolded distributions are then weighted based on the splitting matching hierarchy and summed.

Figure 2 illustrates the fully unfolded distributions of z_g and R_g for jets with $R = 0.4$ in two distinct $p_{T,jet}$ bins. Each color corresponds to a unique split, and the bands surrounding the data points denote systematic uncertainties. Notably, we observe that the splitting tends to become harder and more collinear as the split number increases. Consistent with the preceding section, we note only a weak dependence on $p_{T,jet}$.

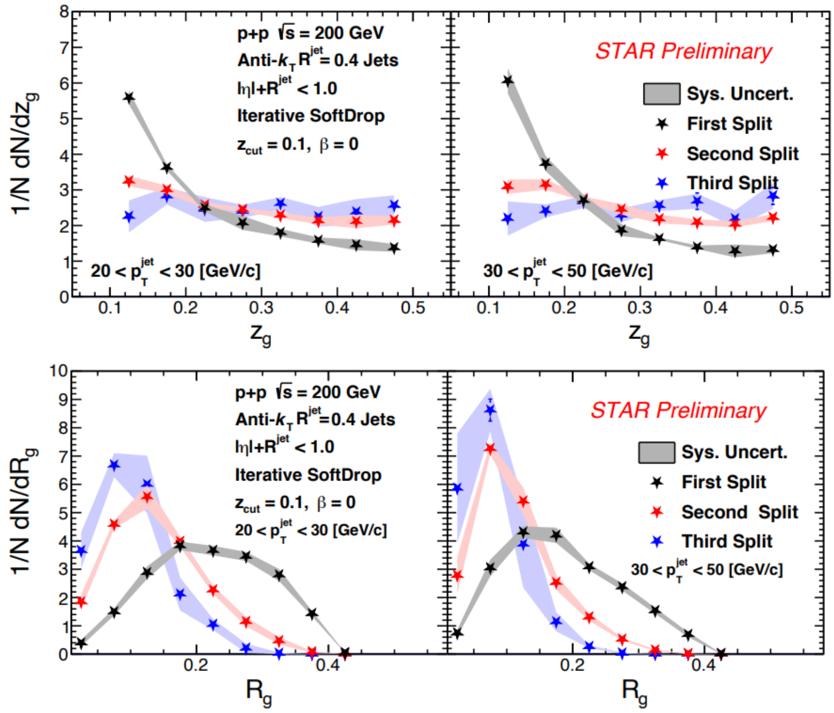

Figure 2. Fully unfolded z_g (top) and R_g (bottom) distributions for different splits of jets with $R = 0.4$ in p+p collisions at $\sqrt{s}$ = 200 GeV. The top and bottom panels are differential in jet p_T for two bins $20 < p_T^{jet} < 30$ GeV/c (left) and $30 < p_T^{jet} < 50$ GeV/c (right).

4. Comparison with different Monte Carlo generators

In Figure 3, we compare the corrected z_g distributions for different R_g (left) and R_g distributions for the first, second, and third splits (right) to predictions from several Monte Carlo (MC) generators. The models considered include PYTHIA 6 [8] with the STAR Perugia tune [9], PYTHIA 8 [10] with the Monash tune based on LHC data [11], and HERWIG 7 [12] with a slightly modified UE-EE-4-CTEQ6L1 tune [13]. These MC models feature distinct implementations of parton shower and hadronization mechanisms. Specifically, HERWIG employs an angular-ordered parton shower, whereas both versions of PYTHIA utilize either k_T or p_T ordering. For hadronization, HERWIG employs the cluster model, while PYTHIA utilizes the Lund string model. In both cases we observe that all MC models capture the overall trend of the data.

5. Conclusions

We have presented comprehensive analyses, including the fully corrected z_g vs. R_g as a function of $p_{T,jet}$ at the first split, and the distributions of z_g and R_g with respect to $p_{T,jet}$ for the first, second, and third splits. Notably, we observe a resemblance between the trends of the z_g distribution at the first split with small R_g and the z_g distribution at the third split which is consistent with angular ordering. Flattering of the z_g distribution is also

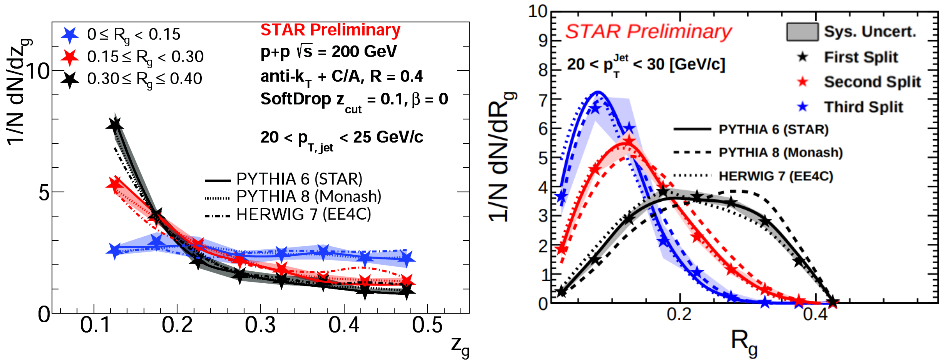

Figure 3. Fully corrected z_g vs. R_g (left) distributions for the first split and R_g distributions for different splits (right) of jets with $R = 0.4$ in p+p collisions at $\sqrt{s}$ = 200 GeV compared with different Monte Carlo generators.

consistent with an evolution to a more non-perturbative regime. Our future investigations will explore correlations involving other substructure observables at the first split, as well as studying z_g and R_g observables for various initiator prong transverse momenta at the first, second, and third splits.

Acknowledgments

The work has been supported by the grant LTT18002 of Ministry of Education, Youth and Sports of the Czech Republic.

1. M. Cacciari et al.. The anti-kt jet clustering algorithm. *JHEP* **2008**, *2008*, 063. https://doi.org/10.1088/1126-6708/2008/04/063.
2. R. Atkin. Review of jet reconstruction algorithms. *Jour. of Phys: Conf Series* **2015**, *645*, 012008. https://doi.org/10.1088/1742-6596/645/1/012008.
3. A. J. Larkoski et al.. Soft Drop. *JHEP* **2014**, *2014*. https://doi.org/10.1007/JHEP05(2014)146.
4. K. H. Ackermann et al.. STAR detector overview. *Nucl. Instrum. Meth. A* **2003**, *499*, 624–632. https://doi.org/10.1016/S0168-9002(02)01960-5.
5. J. Adam et al.. Measurement of Groomed Jet Substructure Observables in p+p Collisions at $\sqrt{s_{NN}}$= 200 GeV with STAR. *Phys. Lett. B* **2020**, *811*, 135846. https://doi.org/https://doi.org/10.1016/j.physletb.2020.135846.
6. G. D'Agostini. A multidimensional unfolding method based on Bayes' theorem. *Nucl. Instrum. Meth. A* **1995**, *362*, 487–498. https://doi.org/10.1016/0168-9002(95)00274-X.
7. F. A. Deyer et al.. Review of jet reconstruction algorithms. *JHEP* **2018**, *2018*. https://doi.org/10.1007/JHEP06(2018)093.
8. T. Sjöstrand et al.. PYTHIA 6.4 physics and manual. *Journal of High Energy Physics* **2006-05-01**, *2006*, 026–026. https://doi.org/10.1088/1126-6708/2006/05/026.
9. P. Z. Skands. Tuning Monte Carlo generators. *Physical Review D* **2010**, *82*. https://doi.org/10.1103/PhysRevD.82.074018.
10. T. Sjöstrand et al.. An introduction to PYTHIA 8.2. *Computer Physics Communications* **2015**, *191*, 159–177. https://doi.org/10.1016/j.cpc.2015.01.024.
11. P. Skands et al.. Tuning PYTHIA 8.1. *The European Physical Journal C* **2014**, *74*. https://doi.org/10.1140/epjc/s10052-014-3024-y.
12. J. Bellm et al.. Herwig 7.0/Herwig++ 3.0 release note. *The European Physical Journal C* **2016**, *76*. https://doi.org/10.1140/epjc/s10052-016-4018-8.
13. M. Seymour et al.. Constraining MPI models using eff and recent Tevatron and LHC Underlying Event data. *Journal of High Energy Physics* **2013**, *2013*. https://doi.org/10.1007/JHEP10(2013)113.